

TEVATRON HEAVY FLAVOR RESULTS ON B LIFETIMES AND DECAYS AND D ASYMMETRIES

S. DONATI

*University and Istituto Nazionale di Fisica Nucleare,
Edificio C, Polo Fibonacci, Largo B. Pontecorvo, 3, 56127, Pisa, Italy*

We review the most recent CDF and D0 results related to B lifetimes, decays and D asymmetries. CDF has recently measured the mass and lifetime of several ground state b -baryons, including Ξ_b^- , Ξ_b^0 and Ω_b^- , in the decay modes with a J/ψ in the final state, as well as in purely hadronic decay modes. We also report on the CDF measurements of the B_c^+ cross section performed in the $B_c^+ \rightarrow J/\psi \mu^+ \nu$, and of the charm mixing. We present the search for the narrow $X(4140)$ resonance performed by D0, which supports the evidence of existence of this state. We conclude with the D0 searches for direct CP violation in the $B^+ \rightarrow J/\psi K^+$ and $B^+ \rightarrow J/\psi \pi^+$ decay modes and in the $D_s^+ \rightarrow \phi \pi^+$ decay mode.

1 Introduction

B hadrons are abundantly produced at the Tevatron Collider, where the measured b production cross section is $\sigma(B^+) = 2.78 \pm 0.24 \text{ } \mu\text{b}$ for $p_T(B^+) \geq 6 \text{ GeV/c}$ and $|y| \leq 1^1$, and the available energy allows the production of lighter B mesons as well as the heavier Λ_b , Σ_b , Ξ_b and Ω_b hadrons. The challenge is extracting signals from background which are orders of magnitude higher at production. This is achieved with dedicated detectors and triggers.

The CDF II tracker is made of three silicon detectors² and a drift chamber³ located within a solenoidal magnetic field. Particle identification is performed with the measurement of the specific ionisation in the drift chamber and of the time of flight in a specific detector⁴. Segmented electromagnetic and hadronic calorimeters surround the tracking system⁵. The muon detectors⁶ are located outside the central hadron calorimeter. CDF II uses a three-level trigger system. The heart of the L1 trigger is the eXtremely Fast Tracker⁷, the trigger track processor that identifies charged tracks in the drift chamber. The L1 tracks are extrapolated to the calorimeter and to the muon chambers to generate electron and muon trigger candidates. The Online Silicon Vertex Tracker⁸ is part of the L2 trigger. It receives the L1 tracks and the digitised pulse heights on the axial layers of the silicon vertex detector. It links the L1 tracks to the silicon hits and reconstructs tracks with offline-like quality, used to select online the secondary vertices characteristic of the b events in specific triggers. L3 trigger uses a CPU farm which allows to perform an almost offline-quality reconstruction.

The D0 detector⁹ uses an excellent central tracking system which consists of a silicon microstrip tracker and a central fiber tracker surrounded by a solenoidal magnet and provides signals to the Level 2 and Level 3 trigger systems, to select events with displaced vertices from b -quark decay. The D0 calorimeter system consists of three sampling calorimeters (primarily uranium/liquid-argon) and an intercryostat detector. The muon system uses proportional drift tubes, mini drift tubes, and toroidal magnets and provides a coverage to $|\eta| \approx 2.0$.

2 Measurement of B baryon properties at CDF

The Ω_b^- observation was made at D0¹¹ and CDF¹⁰ through the decay chain $\Omega_b^- \rightarrow J/\psi \Omega^-$, where $J/\psi \rightarrow \mu^+ \mu^-$, $\Omega^- \rightarrow \Lambda K^-$, and $\Lambda \rightarrow p \pi^-$. The Ξ_b^- is reconstructed through the similar decay mode $\Xi_b^- \rightarrow J/\psi \Xi^-$, where $J/\psi \rightarrow \mu^+ \mu^-$, $\Xi^- \rightarrow \Lambda \pi^-$, and $\Lambda^- \rightarrow p \pi^-$ as a crosscheck. The updated CDF analysis¹² selects well-measured $J/\psi \rightarrow \mu^+ \mu^-$ candidates, where the two-muon invariant mass is required within 80 MeV/c² of the world-average J/ψ mass. Λ candidates use all opposite charge track pairs with $p_T > 0.4$ GeV/c found in the chamber. The proton (pion) mass is assigned to the track with the higher (lower) momentum, which is correct for the Λ candidates used in this analysis for the kinematics of the Λ decay and the lower limit in the transverse momentum acceptance of the tracking system. The additional tracks are assigned the pion or kaon mass, and $\Lambda \pi^-$ and ΛK^- combinations are identified that are consistent with the decay process $\Xi^- \rightarrow \Lambda \pi^-$ or $\Omega^- \rightarrow \Lambda K^-$. The charged hyperon candidates have an additional fit performed with the three tracks that simultaneously constrains the Λ and Ξ^- or Ω^- masses of the appropriate track combinations and provides the best possible estimate of the hyperon momentum and decay position. A significant background reduction is achieved by requiring the charged hyperon candidates have track measurements in at least one layer of the silicon detector. The shorter lifetime of the Ω^- makes the silicon selection not efficient in compare to the Ξ^- . For this reason silicon detector information on the hyperon track is used when it is available, but it is not imposed as a requirement for the Ω^- selection. The hyperon candidates are combined with the J/ψ candidates by fitting the five-track state with constraints appropriate for each decay topology and intermediate hadron state. The $\mu^+ \mu^-$ mass is constrained to the nominal J/ψ mass, and the hyperon candidate is constrained to originate from the J/ψ decay vertex. The fits that include the charged hyperon constrain the Λ candidate tracks to the nominal Λ mass, and the Ξ^- and Ω^- candidates to the respective nominal masses. b -hadron candidates are required to have $p_T > 6.0$ GeV/c and the hyperon to have $p_T > 2.0$ GeV/c. Figure 1 shows the CDF Ξ_b^- and Ω_b^- mass distributions.

CDF measures a Ξ_b^- mass to be $5794.1 \pm 2.0(\text{stat}) \pm 0.40(\text{syst})$ MeV/c² and the Ω_b^- to be $6051.4 \pm 4.2(\text{stat}) \pm 0.50(\text{syst})$ MeV/c². The systematic errors are due to the uncertainty on the mass scale of the baryons measured with the hyperons in the final state, estimated as the mass difference between the B^0 as measured in the $J/\psi K_s^0$ and the nominal B^0 mass and rescaled for the different energy measured by the tracking system in the two decay modes. A systematic error is due to the dependence of the measured on the alternative assumption to have a constant or an event-by-event mass resolution in the fit. A further systematic is due to the uncertainty on the Ω^- mass. The Ξ_b^- lifetime is measured to be $1.36 \pm 0.15(\text{stat}) \pm 0.02(\text{syst})$ ps and the lifetime of the Ω_b^- to be $1.77^{+0.55}_{-0.41}(\text{stat}) \pm 0.02(\text{syst})$ ps. The systematic errors are due to the treatment of the resolution on the proper decay length in the fit and to the detector mis-alignment.

A second dataset, designed for the collection of heavy flavour decay products through the reconstruction of displaced vertices, is used to provide the first evidence for the process $\Omega_b^- \rightarrow \Omega_c^0 \pi^-$, with $\Omega_c^0 \rightarrow \Omega^- \pi^+$. As a crosscheck of this analysis, also the processes $\Xi_b^- \rightarrow \Xi_c^0 \pi^+$, with $\Xi_c^0 \rightarrow \Xi^- \pi^+$, and $\Xi_b^0 \rightarrow \Xi_c^+ \pi^-$, with $\Xi_c^+ \rightarrow \Xi^- \pi^+ \pi^+$ are reconstructed. CDF measures the Ξ_b^0 mass to be $5791.6 \pm 5.0(\text{stat}) \pm 0.73(\text{syst})$ MeV/c² the Ξ_b^- mass to be $5796.5 \pm 4.7(\text{stat}) \pm 0.95(\text{syst})$ MeV/c² and the Ω_b^- to be $6040 \pm 8(\text{stat}) \pm 2(\text{syst})$ MeV/c², compatible with the measurements performed in the J/ψ decay modes.

3 Measurement of the ratio $\frac{\sigma(B_c^+) \times BR(B_c^+ \rightarrow J/\psi \mu^+ \nu)}{\sigma(B^+) \times BR(B^+ \rightarrow J/\psi K^+)}$ at CDF

The B_c is the bound state of a \bar{b} and c quark. Since the \bar{b} and c quark are much closer in mass than more commonly studied heavy-light mesons, the B_c is an interesting laboratory for studying QCD. In addition, the B_c total width can have significant contributions from the partial widths of the c -quark decay, the b -quark decay, or annihilation of the b and c quarks to a W boson,

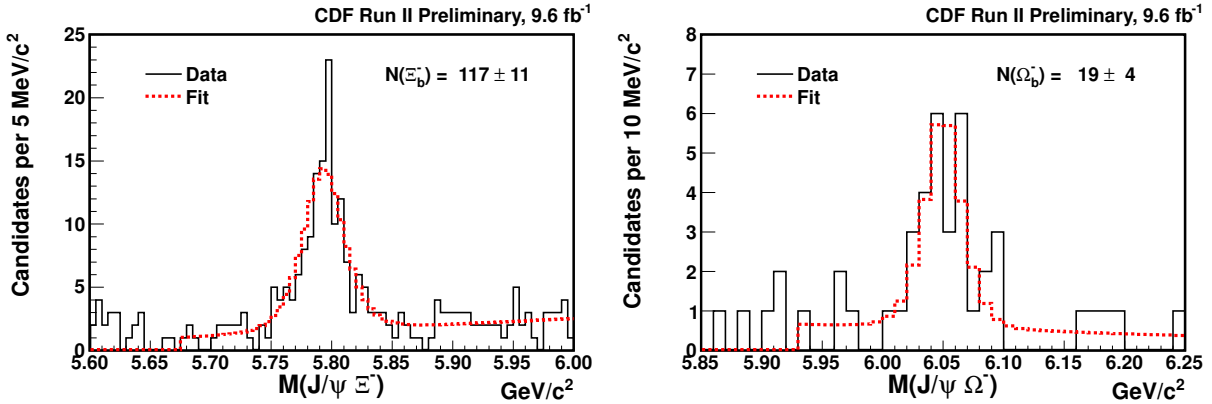


Figure 1 – (Left): The $J/\psi \Xi^-$ and (Right) $J/\psi \Omega^-$ mass distributions used for the CDF b -baryon mass measurements. The probability distributions obtained from the fits are overlaid on the data in dashed red.

in contrast to the light B mesons, where the b quark decay is expected to dominate the width. Since weak decays to a lepton and a neutrino, $b \rightarrow c \bar{\nu}_l$, are common and lead to semileptonic final states with $c \bar{c}$, which can form a J/ψ meson, decays of the B_c through the b quark are of particular interest. For this relative cross section measurement the entire CDF Run II dataset of 8.7 fb^{-1} has been used¹³. Data were collected with the J/ψ di-muon trigger. J/ψ particles are reconstructed through the $\mu^+ \mu^-$ decay channel and are matched to a third track associated with the J/ψ vertex. The third track might be the muon in the $B_c^+ \rightarrow J/\psi \mu^+ X$ decays, or the kaon in the $B^+ \rightarrow J/\psi K^+$ decays, or a pion, a kaon or a proton in the misidentified muon background.

There are 1,370 $B_c^+ \rightarrow J/\psi \mu^+ \nu$ event candidates within 4-6 GeV/c^2 signal mass window and $14,338 \pm 125$ events from $B^+ \rightarrow J/\psi K^+$ decays. The fit function for the $J/\psi K^+$ invariant mass distribution consists of a double Gaussian for $B^+ \rightarrow J/\psi K^+$ decays, a mass template for the Cabibbo suppressed $B^+ \rightarrow J/\psi \pi^+$ contribution within the mass range 5.28-5.40 GeV/c^2 based on Monte Carlo simulation, and a second order polynomial for the continuum background. The Cabibbo suppressed $B^+ \rightarrow J/\psi \pi^+$ contribution is fixed to 3.83 % of the number of $B^+ \rightarrow J/\psi K^+$. The number of B_c^+ signal events is determined by subtracting the background contributions to the sample.

The main sources of backgrounds in the semileptonic B_c^+ sample are misidentified J/ψ , real J/ψ with a misidentified third muon, $b\bar{b}$ background, and contributions from other decay modes. The number of misidentified J/ψ plus a third muon is estimated using the di-muons from the sidebands of the J/ψ mass distribution. We find 11.4 ± 2.4 events below 4 GeV/c^2 , 96.5 ± 6.9 events within the 4-6 GeV/c^2 mass window and 25 ± 3.5 events above 6 GeV/c^2 . The misidentified muon contribution to the B_c^+ background is calculated using a sample of J/ψ -track and by determining the kaon, pion, and proton probability to be misidentified as muons. We have estimated a number of background events with one misidentified muon of $86.7^{+2.4}_{-4.2}$ in the mass region below 4 GeV/c^2 , $344.4^{+9.6}_{-16.5}$ in the 4-6 GeV/c^2 mass region, and $32.1^{+0.9}_{-1.5}$ above 6 GeV/c^2 . The $b\bar{b}$ background accounts for cases when the J/ψ is produced by a b hadron and the third muon is produced by a \bar{b} , or viceversa, in the same event. The $b\bar{b}$ background calculation is based on a PYTHIA Monte Carlo simulation. There is a residual contribution from other B_c^+ decay modes, for example, a B_c^+ might decay into $\psi(2S) \mu^+ \nu$, followed by $\psi(2S)$ decay into J/ψ . Another example is a B_c^+ decay into $J/\psi \tau^+ \nu$ followed by the τ decay into a muon. The probability of events from these decays to survive our selection requirements is small, but non-zero. The number of B_c^+ is obtained by subtracting the backgrounds from the reconstructed candidates, and is reported in Table 1.

The ratio of the production cross section times branching fraction of the $B_c^+ \rightarrow J/\psi \mu^+ \nu$ relative to the $B^+ \rightarrow J/\psi K^+$ can be written as

Table 1: Summary of the misidentified J/ψ , misidentified muon, double fake, and $b\bar{b}$ backgrounds measured in the $B_c^+ \rightarrow J/\psi\mu^+\nu$ sample.

	$M \leq 4 \text{ GeV}/c^2$	$4 \leq M \leq 6 \text{ GeV}/c^2$	$M \geq 6 \text{ GeV}/c^2$
$N(B_c^+ \rightarrow J/\psi\mu^+X)$, reconstr.	132 ± 11.5	1370 ± 37.0	280 ± 14.4
Backgrounds			
Misidentified J/ψ	11.5 ± 2.4	96.5 ± 6.9	25 ± 3.5
Misidentified muon	86.7	344.4	32.1
Double fake	-5.1	-19.0	-5.2
$b\bar{b}$	12.4 ± 2.4	178.6 ± 12.4	110.4 ± 10.7
Other decay modes	2.6 ± 0.1	30.0 ± 0.2	0
$N(B_c^+)$	23.9 ± 12.0	739.5 ± 39.6	45.7 ± 18.3

$$\frac{\sigma(B_c^+) \times BR(B_c^+ \rightarrow J/\psi\mu^+\nu)}{\sigma(B^+) \times BR(B^+ \rightarrow J/\psi K^+)} = \frac{N_{B_c^+}}{N_{B^+}} \times \epsilon_{rel} \quad (1)$$

where $N_{B_c^+}$ and N_{B^+} are respectively the number of B_c^+ and B^+ events estimated from data, and ϵ_{rel} is the relative efficiency between the two decay modes estimated from Monte Carlo. ϵ_{rel} is estimated 4.093 ± 0.038 , where the error is statistical only.

The systematic errors are due to the estimates of the background sources and of the relative efficiency. For the relative efficiency, the sources of uncertainty are the uncertainty on the B_c^+ lifetime and production spectrum, on the B^+ production spectrum, and the uncertainties on the detector and trigger simulation. CDF obtains for $p_T \geq 6 \text{ GeV}/c$ and $|y| \leq 0.6$

$$\frac{\sigma(B_c^+) \times BR(B_c^+ \rightarrow J/\psi\mu^+\nu)}{\sigma(B^+) \times BR(B^+ \rightarrow J/\psi K^+)} = 0.211 \pm 0.212(stat.)^{+0.021}_{-0.020}(syst.) \quad (2)$$

4 Observation of $D^0 - \bar{D}^0$ mixing at CDF

CDF has measured the time dependence of the ratio of decay rates for $D^0 \rightarrow K^+\pi^-$ to the Cabibbo-favored decay $D^0 \rightarrow K^-\pi^+$ ¹⁴. The decay $D^0 \rightarrow K^+\pi^-$ can arise from mixing of a D^0 state to a \bar{D}^0 state, followed by a Cabibbo-favored decay, or from a doubly Cabibbo-suppressed decay of a D^0 . The mixing measurement is based on the ratio of $D^0 \rightarrow K^+\pi^-$ to $D^0 \rightarrow K^-\pi^+$ decay rates. This ratio can be approximated^{15 16} as a quadratic function of t/τ , where t is the proper decay time and τ is the mean D^0 lifetime.

$$R(t/\tau) = R_D + \sqrt{R_D} y'(t/\tau) + \frac{x'^2 + y'^2}{4}(t/\tau)^2 \quad (3)$$

A signal of 3.3×10^4 $D^{*+} \rightarrow \pi^+ D^0$, $D^0 \rightarrow K^+\pi^-$ decays is obtained with D^0 proper decay times between 0.75 and 10 mean D^0 lifetimes. The analysis assumes CP conservation and measures the mixing parameters to be $R_D = (3.51 \pm 0.35) \times 10^{-3}$, $y' = (4.3 \pm 4.3) \times 10^{-3}$, and $x'^2 = (0.08 \pm 0.18) \times 10^{-3}$. Table 2 compares the current CDF result with previous results.

5 Search for the X(4140) state in $B^+ \rightarrow J/\psi\phi K^+$ decays at D0

The X(4140) state²¹ is a narrow resonance in the $J/\psi\phi$ system produced near threshold. The CDF Collaboration reported the first evidence²² for this state and measured the invariant mass and width. The Belle Collaboration searched for X(4140) in two processes and found no signal²³. The resulting upper limit on the production rate does not contradict the CDF measurement.

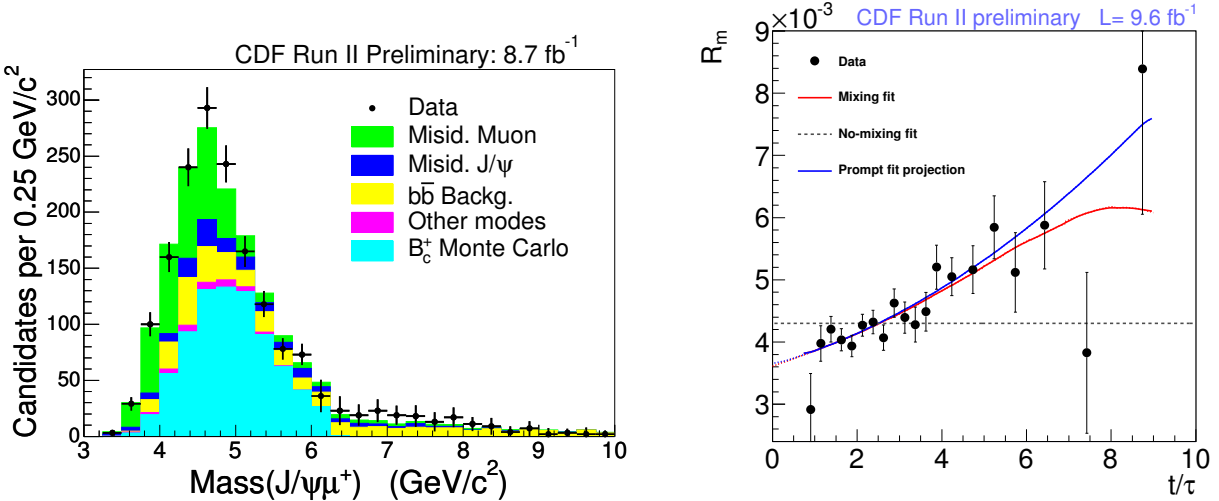


Figure 2 – (Left): Invariant mass distribution of the $B_c^+ \rightarrow \mu^+ \nu$ candidate events with the Monte Carlo simulated signal sample and superimposed. The backgrounds include the misidentified muon (green), the misidentified J/ψ (dark blue), the $b\bar{b}$ backgrounds (yellow), and the other B_c^+ decay modes (pink). The B_c^+ experimental excess is shown as the B_c^+ Monte Carlo (light blue); (Right): Measured ratio R of wrong-sign to right-sign D^* decays as a function of normalised proper decay time. The results of a least-squares fit are shown. A fit assuming no mixing is clearly incompatible with the data.

Table 2: Mixing parameter results and comparison with previous measurements. All results use $D^0 \rightarrow K^+ \pi^-$ decays and fits assuming no CP violation. The uncertainties include statistical and systematic components. The significance for excluding the no-mixing hypothesis is given in terms of the equivalent number of Gaussian standard deviations σ .

Expt.	$R_D(10^{-3})$	$y'(10^{-3})$	$x'^2(10^{-3})$	$\sigma(\text{no mix.})$
CDF(2013) ¹⁴	3.51 ± 0.35	4.3 ± 4.3	0.08 ± 0.18	6.1
Belle ¹⁸	3.64 ± 0.17	$0.6^{+4.0}_{-3.9}$	$0.18^{+0.21}_{-0.23}$	2.0
<i>BABAR</i> ¹⁹	3.03 ± 0.19	9.7 ± 5.4	-0.22 ± 0.37	3.9
CDF(2008) ¹⁷	3.04 ± 0.55	8.5 ± 7.6	-0.12 ± 0.35	9.1
LHCb ²⁰	3.52 ± 0.15	7.2 ± 2.4	-0.09 ± 0.13	9.1

At the LHC, the LHCb and CMS Collaborations have searched for the state. While the LHCb Collaboration found no evidence²⁴, the CMS Collaboration preliminary results²⁵ support the CDF Observation. The quark model does not predict a hadronic state at this mass and several hypotheses have been made on its nature.

Events used in this D0 analysis are collected with single-muon and dimuon triggers, which have different p_T thresholds. Candidate events are required to include a pair of oppositely charged muons accompanied by three additional charged particles with transverse momenta above 0.7 GeV/c. To form B^+ candidates, muon pairs with an invariant mass consistent with the J/ψ mass are combined with pairs of oppositely charged particles, assigned the kaon mass hypothesis, with an invariant mass consistent with the ϕ mass, and a third track, also assigned the kaon mass hypothesis. To suppress the background, cuts on the B^+ transverse decay length, transverse momentum, and impact parameter, are applied. The estimated $B^+ \rightarrow J/\psi \phi$ signal is 215 ± 37 events.

Figure 3 (right) shows the invariant mass distribution of the $J/\psi \phi$ candidates within the B^+ and ϕ mass windows. The significance of the threshold structure is estimated by performing a binned least-squares fit of the B^+ yield to a sum of a resonance and a phase-space con-

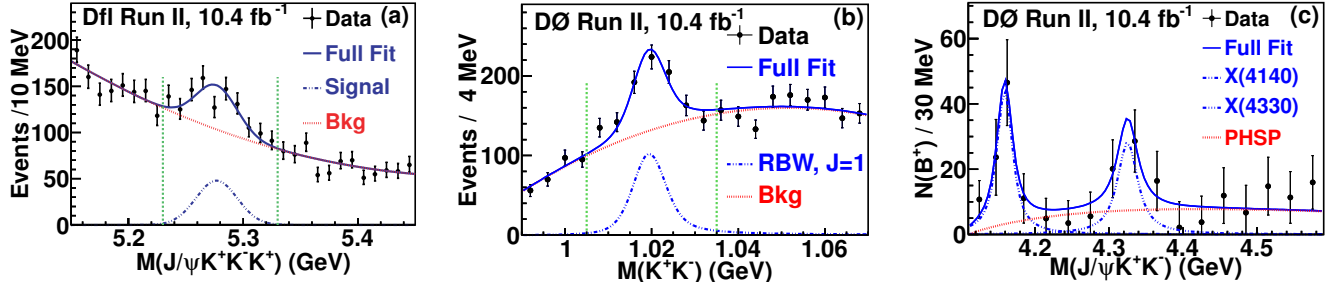


Figure 3 – same figure with draft option (left), normal (center) and rotated (right)

tinuum template. A relativistic Breit-Wigner signal shape is assumed, with mass and width allowed to vary, convoluted with the detector resolution of 4 MeV from simulation. The estimated signal is 52 ± 19 events. The statistical significance of the $X(4140)$ is 3.1σ , with a measured mass of $4159.0 \pm 4.3(\text{stat}) \pm 6.6(\text{syst})$ MeV/c 2 and a width of $19.9 \pm 12.6(\text{stat})^{+1}_{-9}(\text{syst})$. The relative branching fraction $\text{BR}(B^+ \rightarrow X(4140)K^+)/\text{BR}(B^+ \rightarrow J/\psi\phi K^+)$ is measured to be $19 \pm 7(\text{stat}) \pm 4(\text{syst})$ %²⁶.

6 Measurement of the direct CP-violation in $B^\pm \rightarrow J/\psi K^\pm$ and $B^\pm \rightarrow J/\psi\pi^\pm$ at D0

Currently all measurements of CP violation have been consistent with the presence of a single phase in the CKM matrix. The standard model predicts that for $b \rightarrow s\bar{c}\bar{c}$ decays, the tree and penguin contributions have the same weak phase, and thus no direct CP violation is expected in the decays of B^\pm mesons to $J/\psi K^\pm$. Estimates of the effect of penguin loops²⁷ show that there could be a small amount of direct CP violation of up to 0.3 %. A measurement of relatively large asymmetry would indicate the existence of physics beyond the standard model²⁸. Since in the transition $b\bar{d}c\bar{c}$, the tree and penguin contributions have different phases, and there may be measurable levels of CP violation in the decay $B^\pm \rightarrow J/\psi\pi^\pm$ ²⁹.

The analysis reconstructs the two decay modes $B^\pm \rightarrow J/\psi K^\pm$ and $B^\pm \rightarrow J/\psi\pi^\pm$ and measures raw asymmetries by simply measuring the number of B^+ and B^- candidates. The physics CP asymmetry is obtained from the raw asymmetry by applying a correction due to the reconstruction asymmetry between positively and negatively charged kaons in the detector. This is measured using a dedicated sample of $K^{*0} (\bar{K}^{*0}) \rightarrow K^+\pi^- (K^-\pi^+)$, and is found to be (1.046 ± 0.043) %. Other instrumental asymmetries are cancelled by reversing the polarities of the toroidal and solenoidal magnetic fields on average every two weeks, so that the four solenoid-toroid polarity combinations are exposed to approximately the same integrated luminosity. Selection cuts are chosen to minimise the statistical uncertainty of the raw asymmetry in the $B^\pm \rightarrow J/\psi K^\pm$ decay mode.

The asymmetries are measured to be $A^{J/\psi K} = [0.59 \pm 0.36(\text{stat}) \pm 0.07(\text{syst})]$ % and $A^{J/\psi\pi} = [-4.2 \pm 4.4(\text{stat}) \pm 0.9(\text{syst})]$ %. The uncertainties are summarised in Table 3.

7 Measurement of direct CP-violation in $D_s^\pm \rightarrow \phi\pi^\pm$ at D0

Direct CP violation in the Cabibbo-preferred charm decay $D_s^\pm \rightarrow \phi\pi^\pm$ should be non-existent in the standard model, any significant effect in this channel would indicate the existence of physics beyond the standard model. The most recent investigation of this decay by the CLEO Collaboration yields a CP-violating charge asymmetry of $A_{CP} = [0.3 \pm 1.1(\text{stat}) \pm 0.8(\text{syst})]$ %³⁰. The analysis is performed with the full Tevatron Run II data sample with an integrated luminosity of 10.4 fb^{-1} . The $D_s^\pm \rightarrow \phi\pi^\pm$, $\phi \rightarrow K^+K^-$ decay is reconstructed as follows. The two particles from ϕ decay are assumed to be kaons and are required to have $p_T \geq 0.7$ GeV/c, opposite charge and a reconstructed invariant mass compatible with the ϕ mass. The third track is assumed to be a charged pion and is combined with the two previous tracks to create a common

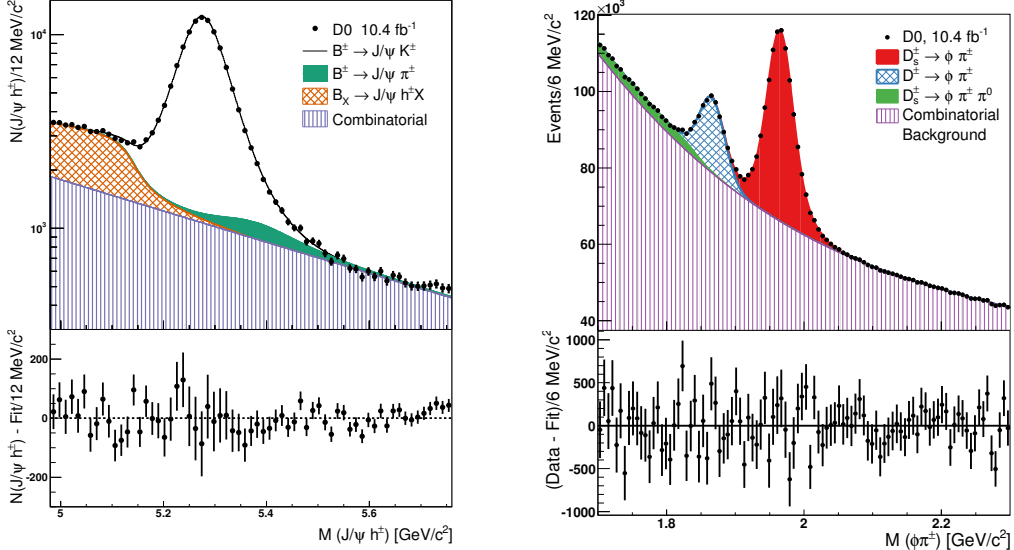


Figure 4 – (Left) Polarity-weighted $J/\psi h^\pm$ invariant mass distribution, where the h^\pm is assigned the charged kaon mass, after all analysis selection cuts. The bottom panel shows the fit residuals; (Right) Polarity-weighted $\phi \pi^\pm$ invariant mass distribution. The lower mass peak is due to the decay $D^\pm \rightarrow \phi \pi^\pm$, while the second peak is due to the D_s^\pm meson decay. The bottom panel shows the fit residuals.

Table 3: The statistical and systematic uncertainties for extracting the the asymmetries $A^{J/\psi K}$ and $A^{J/\psi \pi}$.

Type of uncertainty	$A^{J/\psi K}$ (%)	$A^{J/\psi \pi}$ (%)
Statistical	0.36	4.4
Mass range	0.022	0.55
Fit function	0.011	0.69
Tracking	0.05	0.05
Kaon asymmetry	0.043	n/a
Total systematic uncertainty	0.07	0.9
Total uncertainty	0.37	4.5

D_s^\pm decay vertex. Several variables are used to discriminate between signal and the combinatoric background. The resulting $m(K^+ K^- \pi^\pm)$ is reported in Figure 4 and is used to measure the number of D_s^\pm candidates and a raw CP asymmetry. The total number of D_s^\pm candidates is 451013 ± 1866 . The resulting CP asymmetry, including the corrections due to detector effects and physics effects , is $A_{CP} = [-0.38 \pm 0.26(\text{stat}) \pm 0.08(\text{syst})] \%$ ³¹, which is currently the most precise measurement and is in agreement with the standard model expectation of zero CP violation in this decay.

8 Conclusions

CDF and D0 have been first class players in the field of heavy flavour physics for 20 years, with more than 150 published papers. These results have been complementary and competitive with B-Factories in terms of precision. After showing that precision heavy flavour physics is possible at hadron colliders, we are now leaving a rich legacy to LHC and future B-Factories. We also expect more results from full Tevatron statistics analyses.

References

1. D. Acosta *et al.*, the CDF Collaboration, Phys. Rev. D 75, 012010 (2007); T. Aaltonen *et al.*, the CDF Collaboration, Phys. Rev. D 79, 092003 (2009).
2. A. Sill *et al.*, Nucl. Instrum. Meth. A530:1 (2004).
3. T. Affolder *et al.*, Nucl. Instrum. Meth. A526:249 (2004).
4. D. Acosta *et al.*, Nucl. Instrum. Meth. A518:605 (2004).
5. L. Balka *et al.*, Nucl. Instrum. Meth. A267:272 (1988).
6. G. Ascoli *et al.*, Nucl. Instrum. Meth. A268:33 (1988).
7. E. J. Thomson *et al.*, IEEE Trans. on Nucl. Sc. vol. 49, n. 3 (2002).
8. W. Ashmanskas *et al.*, Nucl. Instrum. Meth. A518: 532, (2004)
9. V. M. Abazov *et al.*, Instrum. Meth. A565: 463, (2006)
10. T. Aaltonen *et al.* (CDF Collaboration), Phys. Rev. D80, 072003 (2009).
11. V. M. Abazov *et al.* (D0 Collaboration), Phys. Rev. Lett. 101, 232002 (2008).
12. T. Aaltonen *et al.* (CDF Collaboration), Phys. Rev. D89, 072014 (2014).
13. CDF Collaboration Public B Group web page, <http://www-cdf.fnal.gov/physics/new/bottom/bottom.html>.
14. T. Aaltonen *et al.* (CDF Collaboration), Phys. Rev. Lett.
15. G. Blaylock, A. Seiden, and Y. Nir Phys. Lett. B 355, 555 (1995).
16. R. Godang *et al.* (CLEO Collaboration), Phys. Rev. Lett. 84, 5038 (2000).
17. T. Aaltonen *et al.* (CDF Collaboration), Phys. Rev. Lett. 100, 12802 (2008).
18. L. Zhang *et al.* (Belle Collaboration), Phys. Rev. Lett. 96, 151801 (2006).
19. B. Aubert *et al.* (BABAR Collaboration), Phys. Rev. Lett. 98, 211802 (2007).
20. R. Aaij *et al.* (LHCb Collaboration), Phys. Rev. Lett. 110, 101802 (2013).
21. J. Beringer *et al.* (Particle Data Group), Phys. Rev. D 86, 010001 (2012); and 2013 partial update for the 2014 edition, <http://pdg.lbl.gov>.
22. T. Aaltonen *et al.* (CDF Collaboration), Phys. Rev. Lett. 102, 242002 (2009).
23. C. Shen *et al.* (Belle Collaboration), Phys. Rev. Lett. 104, 112004 (2010).
24. R. Aaij *et al.* (LHCb Collaboration), Phys. Rev. D 85, 091103 (2012).
25. S. Chatrchyan *et al.* (CMS Collaboration), arXiv:1309.6920.
26. V. M. Abazov *et al.* (D0 Collaboration), Phys. Rev. D 89, 012004 (2014).
27. W.-S. Hou, M. Nagashima, and A. Soddu, arXiv:hep-ph/0605080 (2006).
28. V. Barger, C. W. Chiang, P. Langacker, and H. S. Lee, Phys. Lett. B 598, 218 (2004).
29. I. Dunietz and J. M. Soares, Phys. Rev. D 49, 5904 (1994).
30. J. P. Alexander *et al.* (CLEO Collaboration), Phys. Rev. Lett. 100, 161804 (2008).
31. V. M. Abazov *et al.* (D0 Collaboration), Phys. Rev. Lett. 112, 111804 (2014).